Publ. Astron. Soc. Japan **41**, 373–389 (1989)

The Origin and Behavior of the Background in the Large Area Counters on Ginga and Its Effect on the Sensitivity

Kiyoshi HAYASHIDA, Hajime INOUE, and Katsuji KOYAMA*

Institute of Space and Astronautical Science, 1-1, Yoshinodai 3-chome, Sagamihara-shi, Kanagawa 229

Hisamitsu AWAKI, Shirou TAKANO, and Yuzuru TAWARA

Department of Astrophysics, School of Science, Nagoya University, Furo-cho, Chikusa-ku, Nagoya 464-01

O. Rees WILLIAMS, Michael DENBY, Gordon C. STEWART, and Martin J. L. TURNER

X-Ray Astronomy Group, Department of Physics, University of Leicester, University Road, Leicester, LE1 7RH, U.K.

and

Kazuo MAKISHIMA and Takaya OHASHI

Department of Physics, The University of Tokyo, 3-1, Hongo 7-chome, Bunkyo-ku, Tokyo 113

(Received 1988 October 12; accepted 1989 February 23)

Abstract

The origin and behavior of background in the Large Area Counter on Ginga is discussed and methods of background estimation are described. The size of residual systematic uncertainty in the background, after subtraction, is given, and its effect on the sensitivity of the instrument is discussed. At low energies the sensitivity of the LAC is limited mainly by confusion due to undetectable faint sources in the $1^\circ \times 2^\circ$ field of view: the 3σ level of this source confusion noise is $\sim 6 \times 10^{-12}$ erg cm^{-2} s^{-1} in the 2–10-keV range.

Key words: Instruments; X-ray astronomy; X-ray background.

1. Introduction

The Large Area proportional Counter (LAC) is the main instrument on the third Japanese X-ray astronomy satellite Ginga (Makino and the ASTRO-C team 1987). It

* Present address: Department of Astrophysics, School of Science, Nagoya University, Furo-cho, Chikusa-ku, Nagoya 464-01.

comprises eight collimated proportional counters with a total effective area of 4000 cm^2 covering the energy range 1.5 to 37 keV. The collimator has a $1° \times 2°$ field of view (FWHM). A full description of the LAC is given in the preceding paper (Turner et al. 1989). The large effective area of the LAC enables the determination of the energy spectrum in the band 1.5–37 keV for sources fainter than have hitherto been accessible; the major limitation is the systematic error in background subtraction, rather than source counting statistics.

The LAC background consists of the cosmic diffuse X-ray background falling within the field of view of the collimator, the internal background generated by charged particles and gamma-rays forming the local radiation environment, and by cosmic diffuse X-rays leaking through the detector walls. In addition, for some orientations of the spacecraft, occasional contamination of observations can occur due to solar X-rays scattered into the collimator. The internal background generated by charged particles and gamma rays is reduced by the use of a guard counter surrounding the signal wires, and by inter wire anticoincidence. The background contribution from diffuse X-rays is reduced by shielding the LAC detectors with tin, 0.2 mm thick, placed so as to cover all directions other than the field of view of the collimator. Solar contamination can be avoided by keeping the angle between the LAC field of view and the sun greater than 90°.

In this paper we describe the origin and behavior of the residual internal background in the LAC together with methods of estimation and their uncertainties. The source confusion noise and the effect of fluctuations in the diffuse X-ray background are evaluated and the limiting sensitivity of the LAC is derived.

2. The LAC Background

The LAC is made up of eight identical detectors each of which is provided with its own anticoincidence, internal guard counters and housekeeping monitoring channels. There are two separate X-ray sensing layers identified in the data as top and middle. The top layer is sensitive to X-rays in the 1.5–37-keV band, while the middle layer is sensitive in the range 8–37 keV; it has twice the stopping power of the top layer. The behavior of the background in the two layers is not identical because of differing guard and anticoincidence conditions.

The in-orbit internal background varies with time in a complex fashion; figure 1 shows a typical Ginga observation in the 2–10-keV band. The first 2 days are used for a source observation, and the remainder is for a background (source free) observation. The periods in which the flux in the top layer drops to 10–20 counts s^{-1} correspond to occultation by the Earth of the source and/or the diffuse cosmic X-ray background. Periods of high background occur every $\sim$24 hr and correspond to orbits which pass through the South Atlantic Anomaly (SAA). (The LAC is switched off by a 1-cm^2 solid sate electron detector, SOL2, while it is in the SAA.) As the satellite emerges from the SAA the background declines on a short ($\sim$1 hr) and a long ($\sim$10 hr) time scale. Due to the location of the ground station, satellite contacts always occur during regions of high background, thus orbits are frequently referred to as "contact orbits" (high background) and "remote orbits" (low background). The LAC internal background

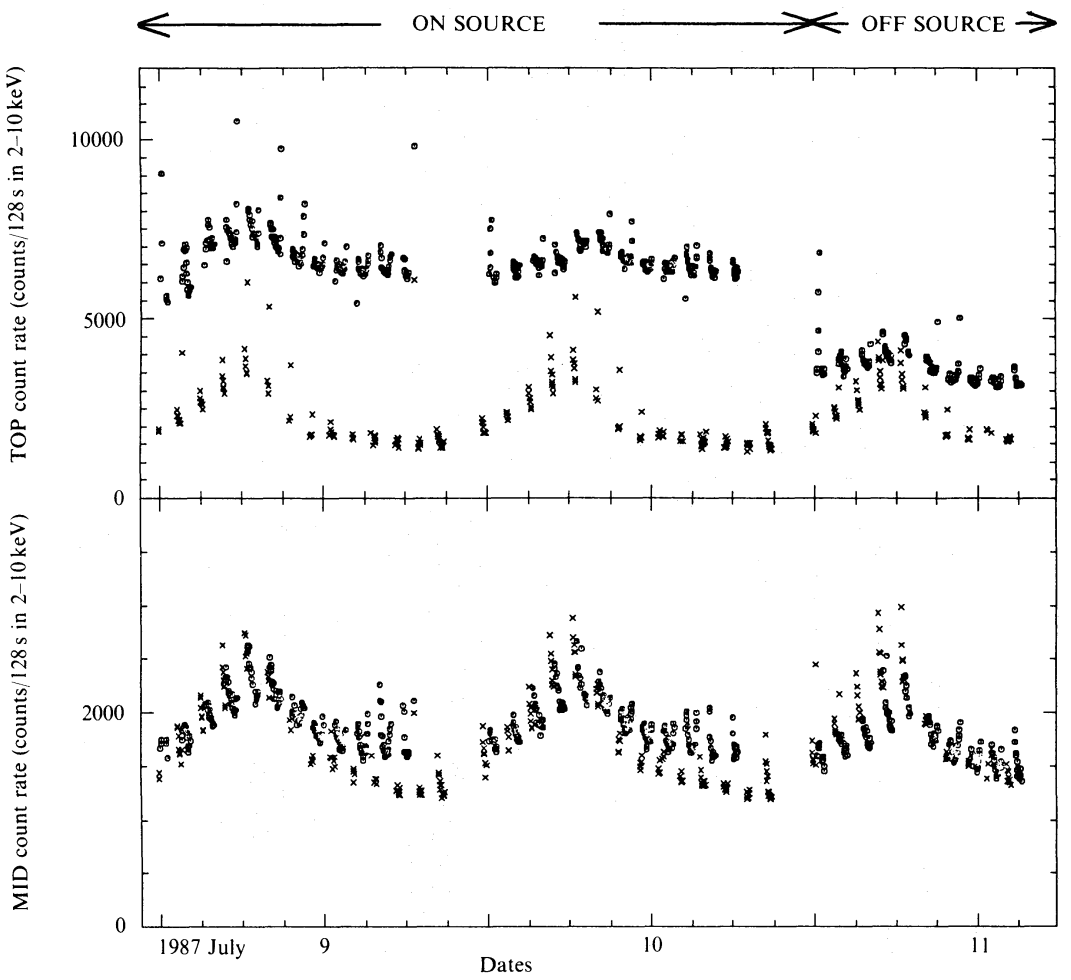

Fig. 1. A typical Ginga observation in the 2–10-keV band. For the first 2 days a source is in the field of view, for the remainder the field is source free. The diffuse backgound is present except when the Earth occults the field of view (data in those occultation periods are indicated with crosses).

has a complex spectral shape. Figure 2 shows the pulse-height spectrum of the internal background in the top and mid layers of the LAC: a number of lines and other spectral features are clearly visible.

While the LAC has no direct means of simultaneously monitoring the internal background, there are a number of housekeeping and other count rates, from both the LAC and accompanying instruments on Ginga, which give indirect measurements vital for background estimation. For ease of reference throughout this paper they are listed below under their three letter data identifier; technical details are given in Turner et al. (1989).

SUD: This is the count rate of X-ray-like events whose energy deposit in the LAC exceeds the upper discriminator. It can be used as a measure of the internal background because the detection efficiency for genuine X-rays is very low ($<6\%$) at such high energies. To first order the SUD rate scales linearly with the background (see figure 3). The upper discriminator is set at 24 keV, however, the count rate above the top spectral channel (37 keV) can be directly computed and is used interchangeably in some

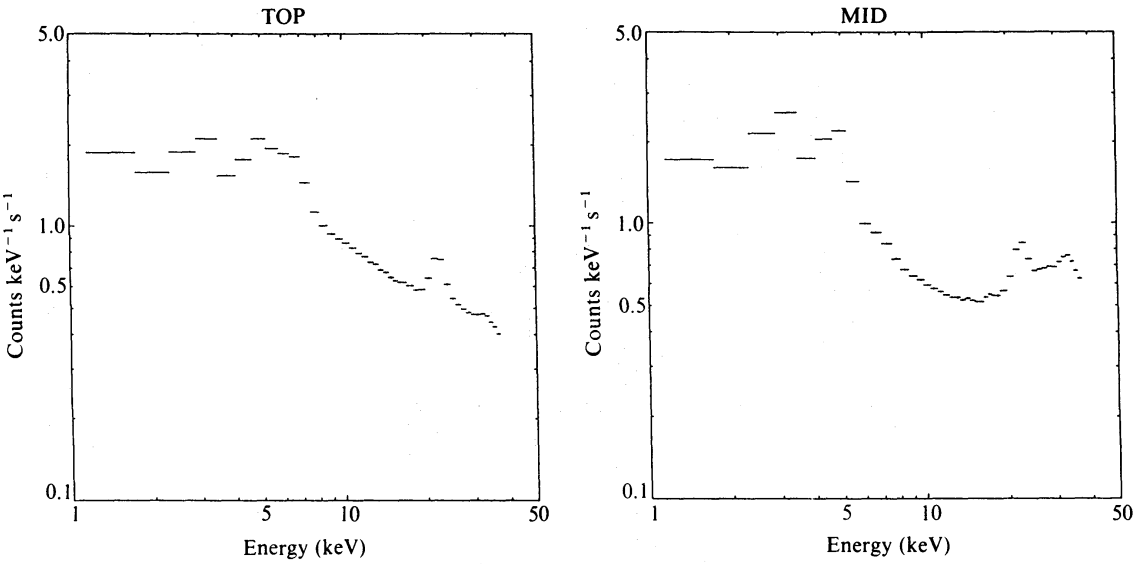

Fig. 2. Pulse-height spectra of a dark Earth observation in top and mid layers of the LAC.

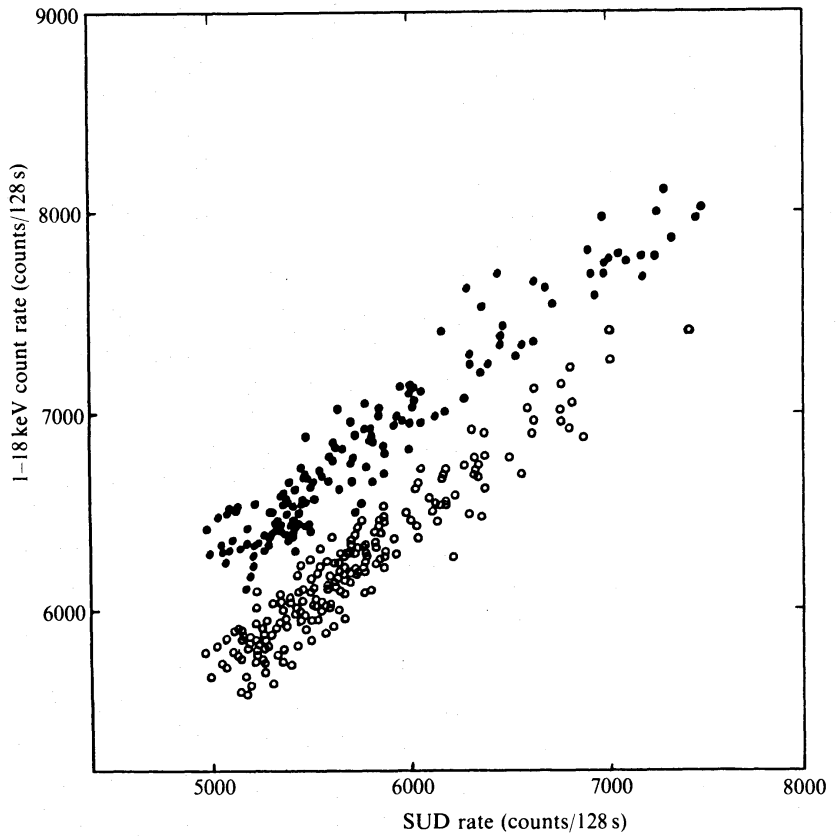

Fig. 3. Relation between 1–18-keV flux and SUD rate in every 128 s for on-source (filled circles) and off-source observations (open circles). The difference in count rate between the two observations is approximately independent of the SUD and is consistent with the source flux.

estimation methods.

PIM: This is the count rate of the LAC sense wires which are screened from direct illumination via the collimator but are otherwise similar to the others. The PIM rate normally scales linearly with the SUD rate, but some conditions cause it to diverge.

MID: The middle layer of the LAC, in the 1–5-keV range, has a low detection efficiency for X-rays (<5%), but it is sensitive to the internal LAC background, and particularly to the 3- and 5-keV line features (see figure 2). The MID rate does not scale linearly with the SUD rate, and provides an important measure of those background components which are not related to the instantaneous external radiation environment.

3. Origin of LAC Background

3.1. Diffuse X-Ray Background

The diffuse X-ray background within the field of view of the LAC generates a count rate of 18 counts s^{-1} summed over the top and mid layers as well as over the full energy range (1.5–37 keV). By contrast, the total background varies from about 70 counts s^{-1} to 150 counts s^{-1}. (For comparison a 1-mCrab source gives about 10 counts s^{-1} in the LAC.) The diffuse flux is constant with time, but fluctuates from point to point over the sky. Its spectrum can be simply estimated by measuring the decrease in the count rate when the sky is occulted by the dark Earth; figure 4 shows the pulse-height spectra attributable to the diffuse X-ray background in the top and mid layers of the LAC. The intrinsic fluctuations in the diffuse X-ray background from place to place on the sky cannot be corrected for and remain as an ultimate uncertainty in the LAC measurements.

3.2. Cosmic Rays

Most minimum ionising particles passing directly through the LAC are rejected,

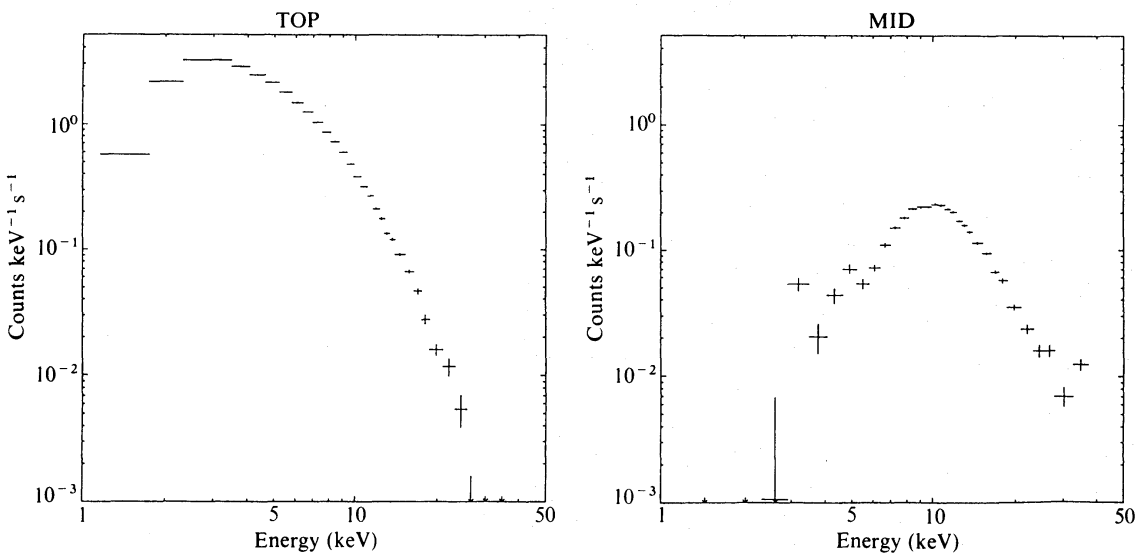

Fig. 4. Pulse-height spectra of the diffuse X-ray background in the top and mid layers of the LAC.

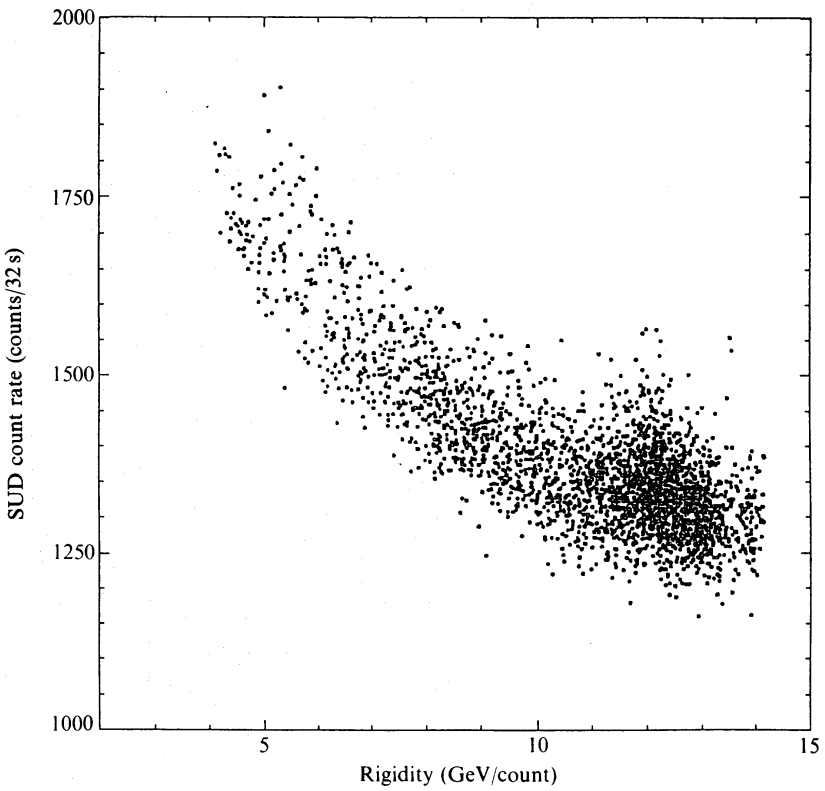

Fig. 5. The variation of the SUD rate against the cosmic-ray cutoff rigidity, for data several hours after passage through the South Atlantic Anomaly.

either by the guards, or because they are detected in both the mid and top layers or in adjacent anodes in the top layer (Turner et al. 1989). Charged particles can, however, contribute to the internal background via Compton interactions of gamma-rays produced in material outside the detector volume by nuclear or electromagnetic interactions.

The cosmic charged particle flux varies with the satellite position, depending on the energy required for a charged particle to penetrate to that position through the Earth's magnetosphere. The charged particle cutoff rigidity (COR) is an estimate of the momentum per elementary unit charge which a particle must have to penetrate from infinity to any given point in the Earth's magnetosphere. Figure 5 shows the SUD rate plotted against COR, for orbits which do not pass through the SAA. The anticorrelation of the SUD rate (rate hence of the background rate) with COR is clearly visible. Some of the variation in figure 5 may be due to sources other than cosmic rays. Since the integrated energy flux of cosmic rays reaching the satellite is a power law function of the COR, we would expect the relation SUD vs. COR to follow a similar law. In fact the time variation of the radioactive background component (see below) sometimes mimics a rigidity dependence. Thus the index of the power law appears to vary from time to time between -0.8 to -1.2. Where this dependence is used in background estimation it is normally assumed to be -1.

3.3. *Geomagnetically Trapped Charged Particles*

Geomagnetically trapped particles contribute to the LAC background in a variety

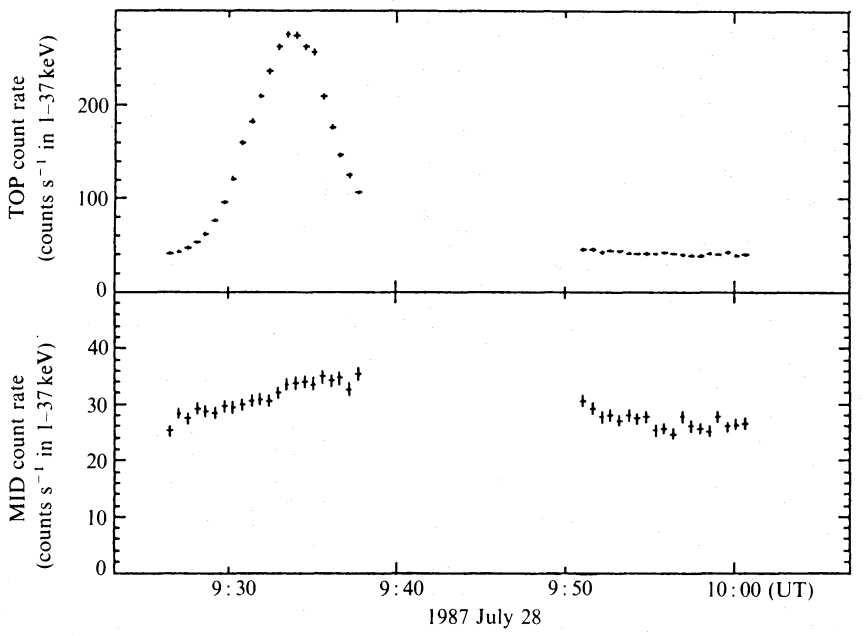

Fig. 6. A soft particle "flare" as seen only in the top layer of the LAC.

of ways. Higher energy particles penetrate the LAC and behave like the cosmic rays; protons undergo nuclear interactions in the material of the LAC and the spacecraft, generating gamma rays; and trapped electrons can penetrate the LAC via the collimator and window, or generate X- and gamma-rays in nearby material. Those soft particles penetrating the collimator and window give rise to signals in the top layer of the LAC only.

The trapped component varies with satellite position, satellite attitude, time and solar activity; it varies over a wide range showing an increase of approximately 5 orders of magnitude while the satellite is passing through the SAA.

There are some unpredictable periods of high background that appear to be associated with soft electrons precipitating from the radiation belts. Figure 6 shows such a soft particle "flare" as seen in the top layer of the LAC. These periods have the following features: the LAC count rate increases in the top layer only; the angle between the geomagnetic field line and the LAC pointing direction is 90°; there is an increase in the SOL2 count rate; and the relationship between the SUD and PIM rates becomes abnormal. These periods cannot be modelled adequately, but need to be rejected ab initio, using one or more of the above characteristics.

3.4. Fluorescence

The line features at 3.1, 6.4, and 22 keV in the background spectrum (see figure 2) are partly due to fluorescent X-rays emitted from the steel collimator (6.4 keV), and from the silver coating (3.0 and 22.1 keV) used to reduce the iron fluorescence (Turner et al. 1989). There are also fluorescent lines from Argon K (3.0 keV), Xenon K (29.6 keV) and Xenon L (4.8 keV), which originate from interactions in the "dead regions" of the LAC (Turner et al. 1989).

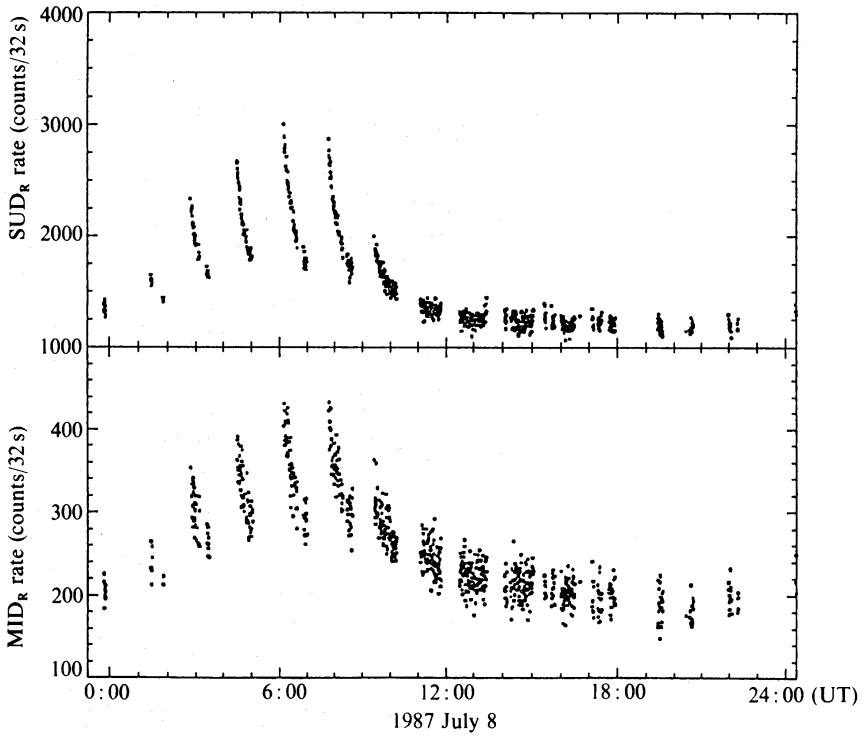

Fig. 7. Time variation of SUD_R and MID_R, the SUD and MID rates after subtraction of the COR related component.

3.5. *Radioactive Decays*

The increased background encountered as the satellite makes an SAA passage persists for a considerable time after emergence, and shows a characteristic exponential decay with time. This is thought to be due to the creation of radioactive isotopes in the material of the spacecraft, and in the LAC, by protons in the SAA. The decaying isotopes contribute to the LAC background probably via Compton interactions of nuclear gamma-rays.

This persistent excess can clearly be seen in the SUD and MID rates, particularly if their COR dependent components have been removed; see, for example, figure 7. The residual SUD rate, SUR_R, is defined as $SUD - m \times COR^{-1}$ after fitting the power-law expression, $m \times COR^{-1}$, to the data shown in figure 5. An analogous rate MID_R can be created by subtracting a COR related component from the MID rate.

Fitting the data shown in figure 7 requires three exponentially decaying components with the characteristic decay times (half lives) of 5.5 min, 41 min, and 8 hr, together with a constant. The presence of the 8-hr component is more clearly seen in the MID_R rate than in the SUD_R rate. This is due to a prominent line feature at about 5 keV in the 8-hr components as seen in figure 8. Figure 8 shows pulse height spectra in the mid layer of the cosmic ray, the 41-min, and the 8-hr components.

The correct estimation of the 8-hr component is very important in the background subtraction, since an inaccurate subtraction would create a false line structure around 5 keV. Then, we must take account of a 37-d periodicity in the LAC background. The satellite orbit is elliptical, with an eccentricity of 0.01 and apogee and perigee heights

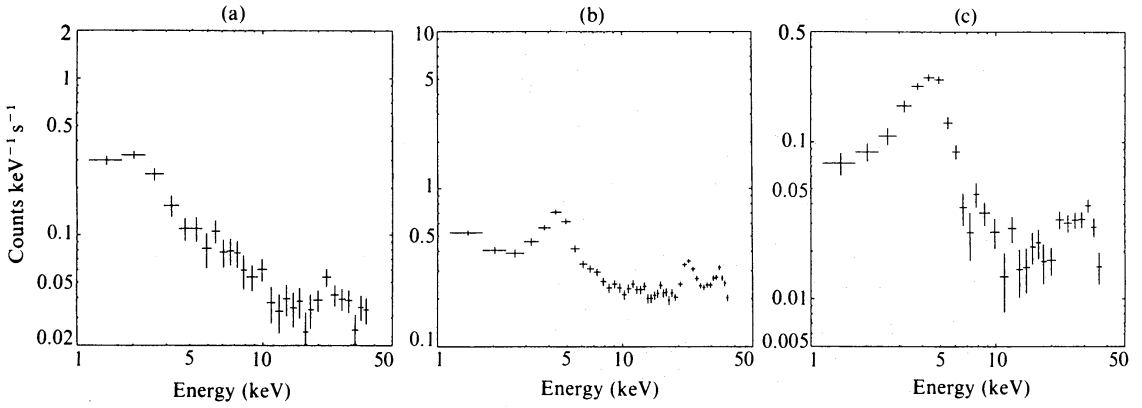

Fig. 8. Pulse-height spectra in the mid layer of the cosmic-ray component (a), the 41-min decaying component (b), and the 8-hr decaying component (c). Each spectrum is obtained by subtraction of the background spectrum at the minimum of the respective variation from the spectrum at the maximum.

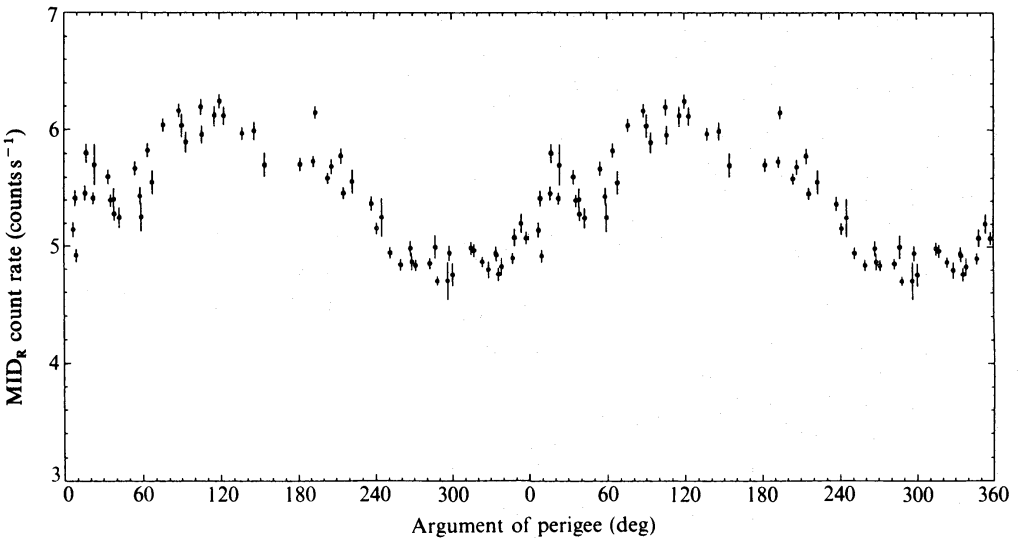

Fig. 9. Variation of the 1–5-keV count rate in the mid layer folded as a function of the argument of the perigee of the satellite orbit. Two cycles are plotted.

of 670 km and 500 km respectively: the altitude at which Ginga passes through the SAA precesses with the orbit at a period of 37 d. The particle flux in the SAA has a strong dependence on altitude, and so the background originating from radioactive decays also has that periodicity. Figure 9 shows the MID_R rate folded as a function of the argument of perigee of the satellite orbit, for data from orbits which do not pass through the SAA. According to the presence of the 8-hr component, the background level in "remote orbits" several hours after the SAA passages still shows the 37-d periodicity. The phase maximum occurs when the satellite passes through the SAA at its highest altitude and experiences the greatest particle flux.

Figure 10 shows the long term evolution of the MID_R rate for a few hundred days after launch. The 37-d cycle is clearly visible, as is a gradual increase with a time scale

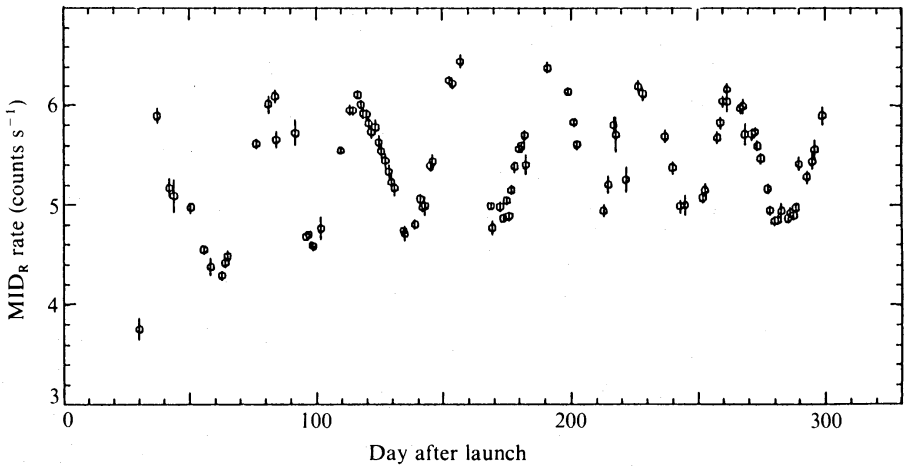

Fig. 10. The long term evolution of the $(MID)_R$ rate for a few hundred days after launch.

of several weeks. This gradual increase can be understood only by the presence of at least one additional decay species which lives longer than tens of days.

From the above it is apparent that there are at least four radioactive components to the background with decay times (half lives) of 5.5-min, 41-min, 8-hr, and tens of days. So far it has not proved possible to identity the isotopes involved. In this paper we concentrate on practical estimates of the contributions to the LAC background from these components. For most purposes the 5.5-min component can be neglected since data close to the SAA are not normally used.

3.6. *Solar Contamination*

When the angle between LAC pointing direction and the sun is less than 90° then contamination of solar X-rays scattered into the collimator can occur, particularly if the sun is in an active state. Figure 11a shows the background subtracted pulse height spectrum of the cluster of galaxies Abell 2218 from data accumulated in the Earth's shadow. Figure 11b shows the same spectrum from data accumulated in sunshine; the angle between the pointing direction and the sun was 85°. An excess in 1–3 keV, due to soft solar X-rays, is clearly visible.

Typically Ginga is only used to study sources where the sun is "behind" the LAC, and so solar contamination is not a problem. In the rare cases where solar contamination is possible its presence can be confirmed by comparing spectra obtained when the satellite is in sunshine with those obtained in the Earth's shadow: alternatively spectra from the LAC modules in the shadow of the solar panels can be compared with those not in the shadow. If solar contamination is found, then only data obtained from the Earth's shadow, or from LAC modules in the shadow of the solar panels can be used, as solar contamination cannot be predicted or estimated post-facto to an acceptable degree of accuracy.

3.7. *Contamination from the Bright Limb of the Earth*

Contamination from the bright limb of the Earth can occur when the angle between the LAC pointing direction and the Earth's horizon angle is less than 0°. Observations should be restricted to times when the horizon angle is $>6°$ because, as for solar

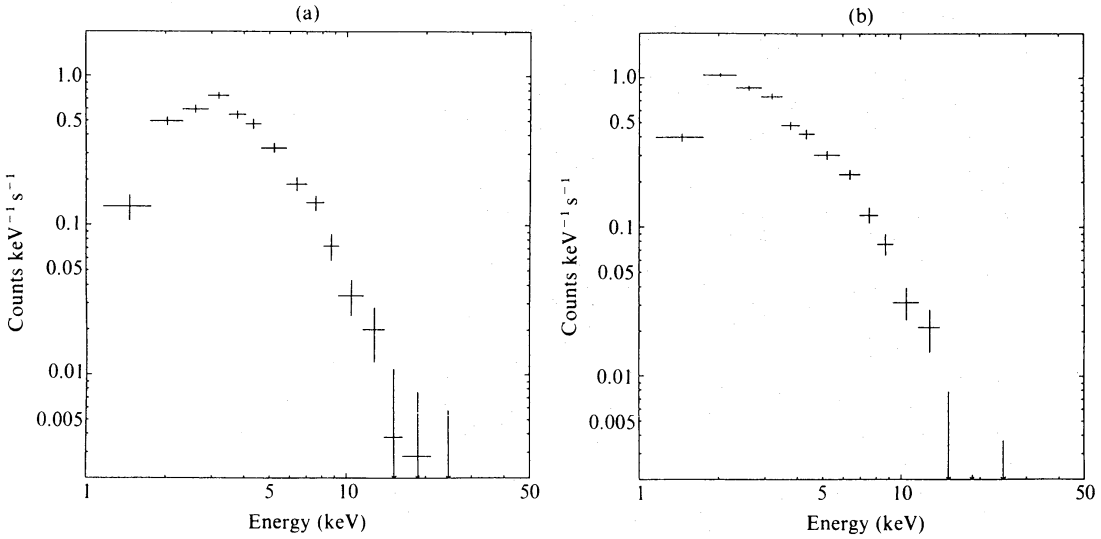

Fig. 11. (a) Background subtracted pulse height spectrum of the cluster A2218. The data was accumulated in the earth shadow. (b) Background subtracted pulse height spectrum of the cluster of galaxies A2218. The data was accumulated in sunshine, and the angle between the LAC pointing direction and the Sun was 85°. An excess in 1–3 keV is clearly visible.

contaminations, this effect cannot be accurately predicted or estimated post factum.

4. Reproduction of the Non-X-ray Background

Simultaneous monitoring of the LAC background during the observation is not possible, so independent background observations have to be made and the data aquired used to give an estimate of the internal background during the source observation. If the various background components mentioned above had the same spectral dependence, then a simple scaling law based for example on the SUD rate could be used to do this. Experience has shown, however, that it is not simply the integral count rate of the internal background which varies with time; the spectrum changes as well (see figure 8). This requires the use of a model containing several independently varying components, each with a unique spectral form.

The modelling method we employ assumes that the intensity of any single component is simply related to one of the housekeeping or environmental parameters, and that this relationship can be determined by independent fitting each energy channel, to source free data thus:

$$C(E, t) = F_1(E) + \sum_{n=2}^{N} P_n(t) \times F_n(E),$$

where

$C(E, t)$ = LAC count rate (as a function of energy and time)
n = label of the component being fitted,
$P_n(t)$ = parameter (as a function of time) being fitted to the data,
$F_n(E)$ = the coefficients (as a function of energy) derived from the fit.

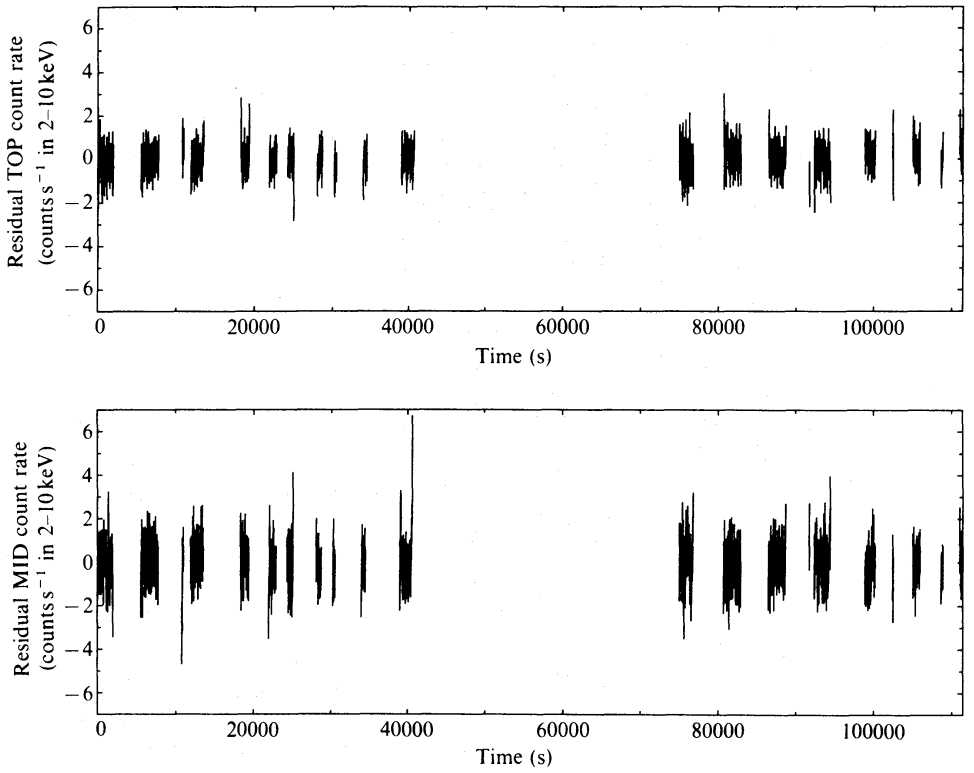

Fig. 12. Residual count rate after subtraction of background from a typical source free observation. The model background was generated using Method I.

The time-independent component, $F_1(E)$, mainly corresponds to the diffuse X-ray background. The time-dependent part consists of a number of components, each with a constant spectral shape and each scaling with a different time-dependent parameter. Once the coefficients have been determined, the same parameters are used to reconstruct an appropriate background for any observation.

4.1. Background Generation from an Adjacent Observation

It has become standard practice for Ginga to devote one day adjacent to the source observation to an observation of source free sky. The background data can be used to determine the background coefficients. The following four parameters have been used frequently in this context (Method I) and are found to be sufficient to reproduce the background data; the SUD rate, the COR dependent component, the 41-min component and the 8-hr component. The SUD is monitored simultaneously with the background observation and the cutoff rigidity is estimated from the satellite position at a given time. For each of the last two terms, we used a "radiation history counter." The path of the satellite is calculated over the period of the observation and for a period of 48 hr preceding this. When the satellite is inside the SAA, the counter is incremented. The counter is allowed to decay exponentially according to the half life of the decay. Figure 12 shows an example of the reproducibility of the internal background by this method. Above model was fitted to a source free observation, and the derived coefficients were used to generate a model background for the same period. The residuals of subtracting this model away from the actual data are plotted in figure 12 as a function of time. All

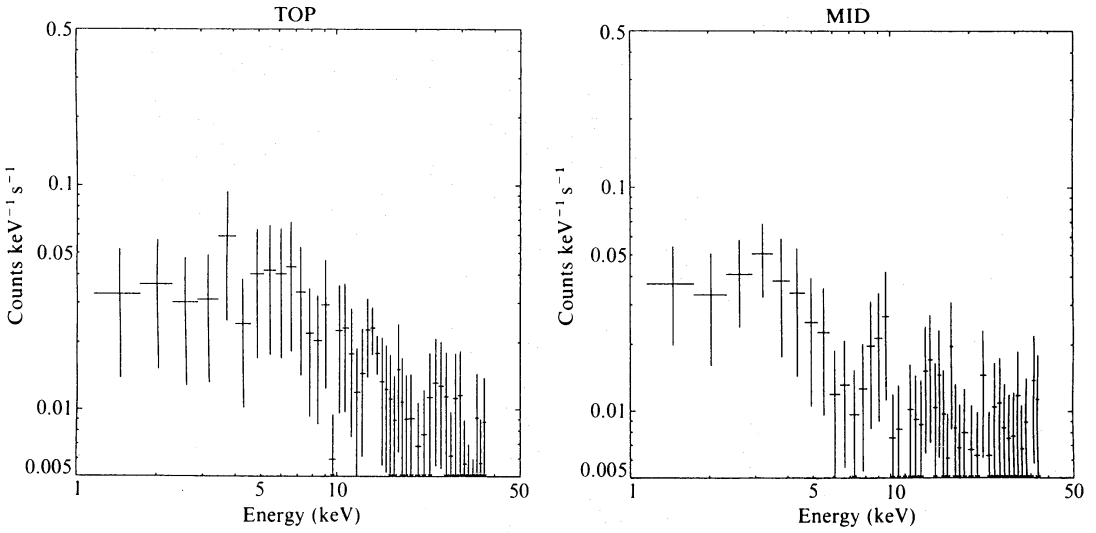

Fig. 13. Root mean squares of residuals after subtraction of model backgrounds by Method I from a number of background data from the same blank sky region.

background data in 128-s bins are well reproduced within the statistical uncertainties.

The accuracy of this technique has been assessed using observations longer than 24 hr in duration. The first 24 hr is used to obtain the background coefficients, and the resulting model background is subtracted from the remainder of the observation, thus we avoid any complications due to the sky to sky variation in the diffuse background. This process has been repeated for four observations. Figure 13 shows the root mean square (RMS) of the residuals of the pulse height spectra after such subtractions and represents the uncertainties in the reproduction of internal background, including the statistical uncertainties.

4.2. *Background Generation from Many Observations*

After an accumulation of background datasets spanning durations exceeding the 37-d cycle, another method has become available (Method II). Four parameters; the SUD rate, the COR related component, the MID rate and a component including the argument of perigee of the satellite orbit are currently used in this method. The last term has a dependency on the argument of perigee (AOP) as $\cos(\mathrm{AOP}-\mathrm{AOP}_0)$, where AOP_0 is the phase at which this term becomes maximum and is empirically found to be 120°. The coefficients are determined so as to fit best to the accumulated background datasets, and a background observation adjacent to each of source observations is not needed in this method.

In order to test this method, two datasets were prepared: one of source free observations near the Large Magellanic Cloud taken between December 1987 and February 1988, and the others of source-free observations at high galactic latitude ($b>15°$) taken between June 1987 and February 1988. Firstly, using the LMC data, coefficients for the time-dependent components were determined. Since the separate observations were all of the same blank sky position, this determination was free of uncertainties due to fluctuations in the diffuse background. Then, the high galactic latitude data (several different pointing directions) were used to determine the average

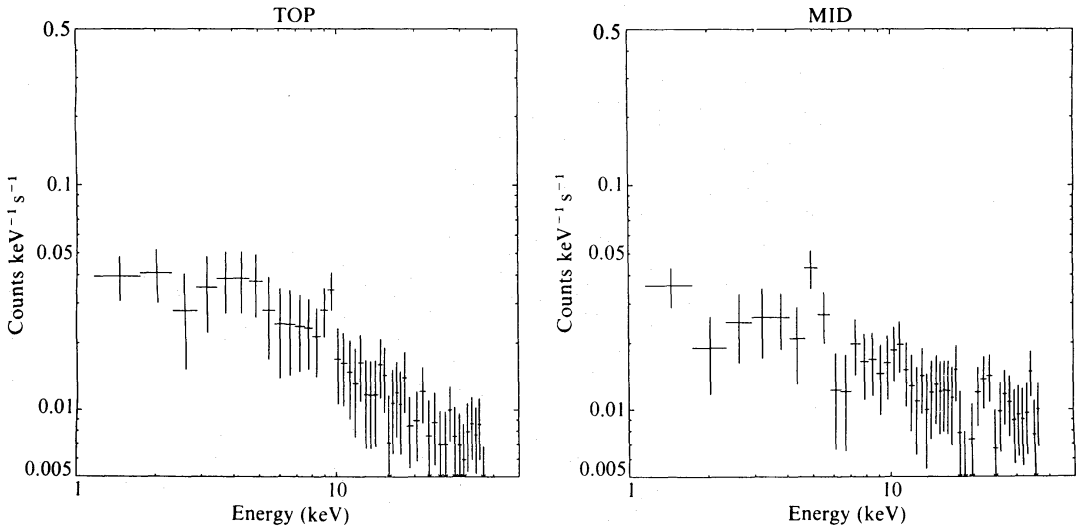

Fig. 14. Root mean squares of residuals after subtraction of model backgrounds by Method II from a number of background data from the same blank sky region.

time-independent background.

The model was used to predict the background spectrum for the individual members of the LMC dataset, and the accuracy of this technique was determined by subtracting the model backgrounds from the actual backgrounds. Figure 14 shows the RMS of the residual pulse height spectra after such subtractions and represents the uncertainties in the reproduction of internal background, including the statistical uncertainties.

4.3. Comparison of Background Subtraction Methods

Both the methods described above can generate an acceptable estimate of LAC backgrounds. Both have a similar degree of accuracy in estimating the internal background of the LAC as seen in figures 13 and 14. The choice depends on the particular circumstances of the observation.

Method II has the attractive advantage that a time consuming background observation need not be made for every observation and also that the statistical accuracy of the background subtracted source spectra is not limited by the length of the background observation. Another advantage of Method II is that the diffuse X-ray background in the generated background is averaged over many different blank sky observations. In Method I, both sky levels in on- and off-source observations fluctuate independently unless the fluctuations have a large scale structure. If we derive the difference of two quantities which are independent but have the same probability distribution, the distribution for the difference will be $\sqrt{2}$ times wider than the original distribution. At low galactic latitudes, where there is a large-scale structure in the diffuse background [e.g. Koyama (1989) and references therein], the method using a nearby source free observation will give a better estimate.

In certain cases, the MID rate cannot be used, and then it is advantageous to use Method I to generate the model background. The parameter MID is only available when the satellite is accumulating data in the MPC1 mode (Turner et al. 1989); separate

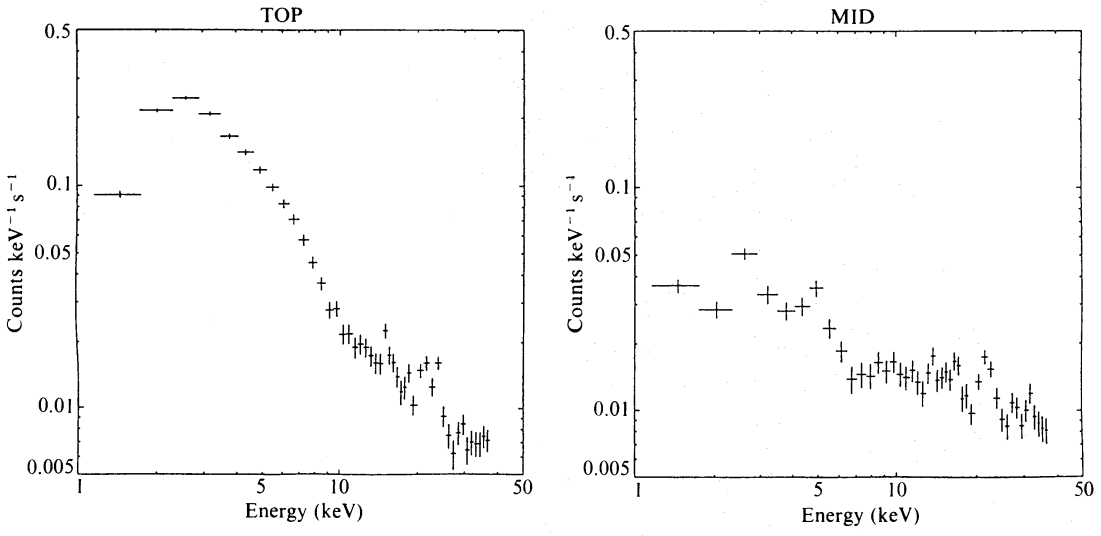

Fig. 15. Root mean squares of residuals after subtraction of model backgrounds from a number of background observations from different sky regions at high galactic latitude.

middle and top layer data are not available in other modes. Even if available, the MID rate cannot be used for sources with a flux stronger than 10 mCrab because the X-ray contribution to this rate cannot be neglected. The use of the PIM rate instead of MID has been investigated, but the accuracy of the background reproduction becomes worse.

5. Sensitivity Limit of the LAC

As discussed in the previous section both methods of estimating the particle background have their merits, and in most cases have a similar degree of accuracy in estimating the internal background of the LAC. The limiting sensitivity of the LAC is not, however, simply the accuracy with which the internal background can be determined. The fluctuation of the diffuse X-ray background from point to point in the sky is important in the 2–10-keV range.

Figure 15 shows the RMS of the residual pulse height spectra after the background subtraction by Method II for a number of fields at high galactic latitude with no known X-ray sources. We can clearly see significant excesses in the RMS distribution in figure 15 as compared to that in figure 14 which are due to the fluctuation of the diffuse X-ray background. The distribution of the residual in the 2–10-keV count rates is shown in figure 16. In this plot, the count rates in the top and mid layers are summed. Then, we calculated the RMS of the distribution as a function of the uppermost count rate of the integration. Since the distribution has a tail extending to the brighter side, in principle, the RMS depends on where we stop the integration. If we select the uppermost boundary so as to correspond to the 3σ level, the 1σ level of the distribution is calculated to be 0.86 counts s^{-1}. The 3σ sensitivity of the LAC in the 2–10-keV band is thus 2.6 counts s^{-1}, corresponding to a flux of about 6×10^{-12} erg cm^{-2} s^{-1} for a Crab-like spectrum.

We estimated the 1σ fluctuation level of the confusion of very faint sources in the

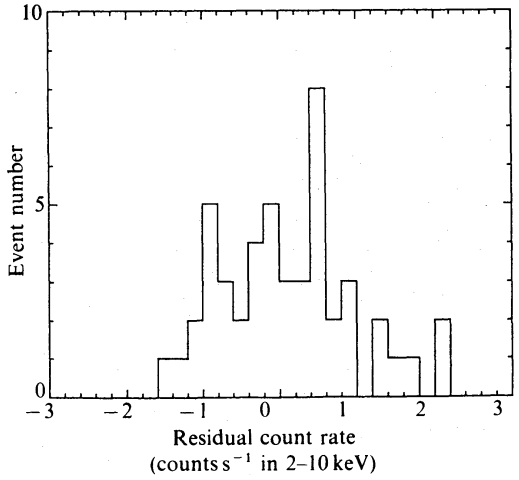

Fig. 16. The distribution of residuals in the 2–10-keV energy band summed over the top and middle layers after the background subtraction from a number of different sky regions.

LAC field of view to be about 0.7 counts s^{-1} using the log N-log S relation determined with HEAO-1 (Piccinotti et al. 1982) by the method of Condon (1974). This suggests that the 2–10-keV sensitivity is limited mainly by the source confusion noise. For observations with the same sky position the integrated residual in the 2–10-keV band is about 0.3 counts s^{-1} (figure 14). If we add this in quadrature to the expected confusion noise, the result gives an estimate of 0.8 counts s^{-1} for sky fluctuations for the pointings with different sky positions. This value is roughly consistent with the value of 0.86 counts s^{-1} obtained from figure 16 within the uncertainties in the above treatment, but we cannot exclude the presence of other components in the sky fluctuations such as large scale structures in the diffuse X-ray background even in the fields at high galactic latitude.

The studies presented here of the background in the LAC leave several areas where further work is necessary, in particular the identification of the radioactive isotopes which contribute to the LAC background. This is important for future missions. Further tests and experiences with background estimation using many datasets are necessary if this is to replace the present rather wasteful devotion of one day per observation to determine the background. We expect to improve the estimation somewhat by optimising the models. However, the methods presented here already give an RMS error on the internal background which is in most cases dominated by the fluctuations in the diffuse background. In this sense we do not expect that the limiting sensitivity of the LAC will be improved beyond that given here.

The authors express their sincere thanks to all members of the Ginga team. This work could not have been realized without their efforts in both hardware and software development, and in the operation and tracking of the Ginga satellite.

Reference

Condon, J. J. 1974, *Astrophys. J.*, **188**, 279.

Koyama, K. 1989, *Publ. Astron. Soc. Japan*, **41**, 665.
Makino, F., and the ASTRO-C team 1987, *Astrophys. Letters Commun.*, **25**, 223.
Piccinotti, G., Mushotzky, R. F., Boldt, E. A., Holt, S. S., Marshall, F. E., Serlemitsos, P. J., and Shafer, R. A. 1982, *Astrophys. J.*, **253**, 485.
Turner, M. J. L., Thomas, H. D., Patchett, B. E., Reading, D. H., Makishima, K., Ohashi, T., Dotani, T., Hayashida, K., Inoue, H., Kondo, H., Koyama, K., Mitsuda, K., Ogawara, Y., Takano, S., Awaki, H., Tawara, Y., and Nakamura, N. 1989, *Publ. Astron. Soc. Japan*, **41**, 345.